

GLOBAL ATMOSPHERIC DENSITY ESTIMATION USING A SEQUENTIAL FILTER/SMOOTHER

James W. Woodburn* and John H. Seago†

Sequential estimation algorithms are applied to the problem of global atmospheric density estimation. An optimal sequential filter is combined with a variable lag smoother to investigate the estimation of corrections to intermediary temperature parameters in the Jacchia 1970 atmospheric density model. Of specific interest are the time lag required to provide the most accurate definitive estimates of temperature corrections, and the observability and correlation associated with several parameterizations of the temperature corrections.

INTRODUCTION

A predominate source of dynamical model uncertainty for low Earth-orbiting (LEO) spacecraft is due to the mis-modeling of atmospheric density at orbital altitudes. The estimation of corrections to global atmospheric models, deduced from the observed behavior of artificial satellites, has moved from an area of research to an operational practice within the space surveillance community.^{1,2,3} Estimated corrections are applied to improve the orbit determination and prediction accuracy for other LEO objects. Objects included in the calibration set are preferably non-maneuvering with nearly constant ballistic coefficients.

The global atmospheric-density-correction model developed and maintained by the US Air Force Space Command (AFSPC) is known as the *High Accuracy Satellite Density Model* (HASDM). HASDM is based on a modified form of the Jacchia 1970 density model which has been extended to utilize corrections to two internal temperature parameters, the nighttime minimum exospheric temperature, T_c , and the inflection point temperature at 125 km altitude, T_x . The process of estimating corrections to the modified Jacchia 1970 model is referred to as the *dynamic calibration of the atmosphere* (DCA).⁴ HASDM also predicts temperature corrections as a function of predicted space weather indices ($E_{10.7}$, a_p).⁵

The estimator used by AFSPC is based on batch weighted least squares (BWLS) algorithms. In BWLS orbit determination, a set of constants are estimated which, along with associated dynamical models, describe the trajectory of the spacecraft. Typical elements of the estimation state include the orbit position and velocity at a fixed epoch, a ballistic coefficient, and a solar pressure coefficient. The period over which observations are processed is called the least-squares *fit span*. When necessitated by temporally changing conditions across the fit span of the BWLS process, state parameters may be estimated as segmented time constants over intervals shorter than the global fit span. In this case, multiple values of the ballistic coefficient, for example, are estimated

* Chief Orbital Scientist, Analytical Graphics, Inc., 220 Valley Creek Blvd., Exton, PA, 19341-2380.

† Astrodynamics Engineer, Analytical Graphics, Inc., 220 Valley Creek Blvd., Exton, PA, 19341-2380

over the fit span, where each segmented estimate has been fit to a shorter, pre-determined time interval. This segmentation procedure allows the state element to approximate a time varying parameter under the restriction that enough data exist over each sub-interval of the fit span to allow for the solution of BWLS normal equations.

In HASDM, corrections to the temperature parameters of the global density are modeled as segmented time constants, as are the so-called *local density compensators* (LDC).³ LDCs are proportional density modifiers used to accommodate local density variations to each satellite which are not predicted by the global model. Temperature-correction estimates for the global atmospheric density model and LDC's are segmented into 3-hour intervals. For non-calibration satellites, ballistic coefficients are estimated as a constant plus a series of segmented constants, where segment lengths can vary between one-half hour and three hours depending on the particular resident space object.²

The purpose of this study is to investigate the potential benefits of applying sequential estimation technology to the problem of global atmospheric density estimation. Sequential estimators have been used to compute corrections to the atmospheric density local to the spacecraft location—similar to LDCs used in HASDM—and to demonstrate simultaneous estimation of ballistic coefficients and local atmospheric density corrections.^{6,7} Estimation of time-varying parameters is supported natively in sequential estimation, requiring no specialized logic or operator involvement. Sequential estimators also eliminate concerns over the tuning of fit spans, eliminate discontinuities in estimated corrections at segment- and fit-interval boundaries, and improve potential computational efficiency. The technology used in this investigation consists of the optimal sequential filter and variable lag smoother implemented in the Orbit Determination Tool Kit (ODTK) product developed by AGI.^{8,9,10} The goals of this effort are:

- to determine the viability of using sequential estimation for generating corrections to global atmospheric density models,
- to analyze the effect of the correction model parameterization on observability and recovery of density errors, and
- to illustrate the relationship between latency and accuracy of the correction estimates.

HASDM estimates corrections to two temperature parameters of the global atmospheric density model, expressed as spherical harmonic expansions in a coordinate system referenced to the direction of the Sun. Previous research has analyzed the correlations between the correction state estimates and investigated the selection of a modified set of temperature parameters to reduce the correlation.³ This study further investigates the presence of such correlations under sequential estimation. In addition, comparisons of lower order correction model parameterizations are made in terms of observability and the ability to provide spatially dependent corrections to the global atmospheric density model.

Timely density information has great operational value. A time lag, relative to real time, may be experienced when estimating corrections to atmospheric density due to the manner in which modeling errors are sensed. HASDM reportedly estimates corrections to atmospheric density based on the observed motions of orbiting objects influenced by atmospheric drag. While drag contributes to the overall acceleration of a spacecraft, Space Surveillance Network (SSN) observations are primarily indicative of the spacecraft position. The local atmospheric density is, therefore, not directly observable; the effects of atmospheric density must integrate from acceleration space into position and velocity space before they can be observed. As a result, density estimates cannot be deduced from tracking data in real time.

The time lag required to reduce the uncertainty of density-correction estimates of is a focus of this study. Specifically, the relationship between the time scales involved in atmospheric density variations and the lag required to achieve full accuracy in the correction estimates is examined using the recently introduced *Variable Lag Smoother* (VLS) which produces improved estimates at historical epochs while running forward in time with the filter.¹¹ The VLS has the desirable characteristic of providing minimum variance estimates at historical epochs based on real time observation processing. The processing of *in-situ* observations—such as space-borne accelerometer measurements—could potentially reduce the latency of density correction estimates in the future, but this is beyond the scope of this study.

CORRECTION PARAMETERIZATIONS

The Jacchia 1970 atmospheric density model is selected as the baseline global density model for this study.¹¹ The Jacchia 1970 model used in this study is not identical to the modified form of the same model used in HASDM, but is sufficiently similar for simulation purposes. A predecessor to HASDM, the Modified Atmospheric Density Model (MADM), also used the Jacchia 1970 model as its baseline.

Corrections to T_c and T_x as Spherical Harmonic Expansions

This study follows the work performed in the development of HASDM, where corrections to the nighttime minimum exospheric temperature, T_c , and the inflection point temperature at 125 km, T_x , are estimated as coefficients of low degree and order spherical harmonic expansions:

$$\Delta T = \sum_n \sum_m C_{n,m} P_{n,m}(\sin \varphi) \cos(m\lambda) + S_{n,m} P_{n,m}(\sin \varphi) \sin(m\lambda) . \quad (1)$$

The corrections are referenced to a coordinate system with the Z axis aligned with the pole of the true equator and the X axis constrained to the direction of the Sun. The corrected temperature parameters drive the computation of density through the physics of the baseline model. This parameterization is implemented and investigated for this study because it is in operational use and therefore allows for the possibility of results comparisons in the future. A zero degree and order expansion (scalar representation) in both temperature corrections is analyzed first, followed by a 1×1 expansion in T_c and finally the operational 1×1 expansion in T_x with a 2×2 expansion in T_c .

SEQUENTIAL ESTIMATION

Sequential estimation techniques are used to estimate the coefficients of the spherical harmonic expansions representing the corrections to the atmospheric density model temperature parameters. Simulated tracking data for a set of low altitude satellites are processed through an optimal sequential filter and VLS.¹⁰ Because atmospheric density errors influence the orbit trajectory through acceleration, there is a lag between when the errors are experienced and when they are observable to the filter through measurements in velocity or position space. As a result, filter estimates of atmospheric density corrections lag, making them undesirable for use in the computation of trajectories of other satellites or for incorporation in regression analyses used to predict future atmospheric corrections. The smoothing process removes the time lag in the estimates.

Time-Varying Estimates

The errors associated with the *a priori* density model result from inaccurate and incomplete knowledge of time-varying atmospheric drivers such as solar and geomagnetic activity. Imperfect physics within the density model also contribute to these errors, and the corrections to the model

will therefore be naturally time varying. While a BWLS algorithm generating segmented time constants can account for the time variation of the density and drag profile mis-modeling, a more innate technique is available via sequential estimation.

The sequential filter implementation in our modified version of ODTK uses exponentially correlated stochastic sequences to represent the correction coefficients for each of the temperature parameters. The resulting estimates can vary over time and are therefore free to reflect changes in the atmosphere as sensed through observations, given an appropriate specification of the error correlation over time. Because each filter/VLS run is started using the final state and state error covariance from the prior filter run, there are no discontinuities in the smoothed estimates resulting from segmentation of the estimation process. There still exists, however, the possibility that discontinuities in the estimates may be required, dependent upon the treatment of the solar flux and geomagnetic indices used to drive the density model. If these inputs are treated as step functions, then discontinuities would be needed in the computed atmospheric density correction parameters to produce a smooth density function. For this reason, we choose to interpolate the input solar flux and geomagnetic indices.¹²

The scalar exponential Gauss-Markov sequence used to represent each temperature correction coefficient is defined as

$$x(t_{k+1}) = \Phi(t_{k+1}, t_k)x(t_k) + \sqrt{1 - \Phi^2(t_{k+1}, t_k)} w(t_k), \quad k \in \{0, 1, 2, \dots\}, \quad (2)$$

where $w(t)$ is a Gaussian white random variable with mean zero and constant variance, σ_w^2 , and

$$\Phi(t_{k+1}, t_k) = e^{\alpha|t_{k+1} - t_k|} \quad (3)$$

where α is a constant less than zero which is related to the half-life, τ , of the sequence via

$$e^{\alpha\tau} = \frac{1}{2} \quad (4)$$

$$\alpha = \frac{\ln(1/2)}{\tau} \quad (5)$$

This sequence is well suited for the estimation of corrections to an *a priori* model in that the expected value of the correction goes to zero and the variance returns to a constant initial value in the absence of measurements. The rate at which estimates decay to zero is controlled through the specification of the parameter half-life. The specification of an infinite half-life would cause a parameter to behave as a time constant while the specification of a zero half-life results in a Gaussian white noise process. When processing real data, half-life values are determined by observing the behavior of estimates during an initial calibration exercise. For the purposes of simulation, half-life values are typically selected based on the time scales of the physical processes being analyzed. Exponential half-lives can be set independently for each estimated parameter allowing each to evolve at its own rate. Figure 1 shows simulated temperature correction behaviors using half-lives of three hours and one day.

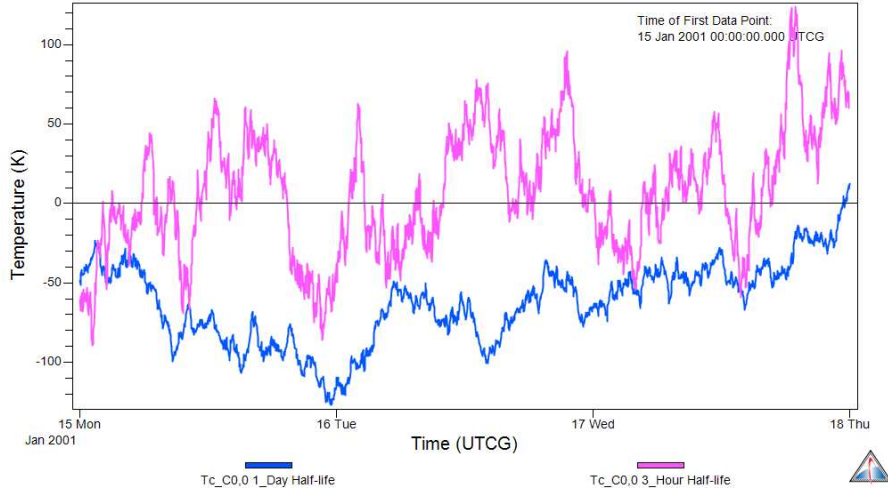


Figure 1. Simulated temperature correction profiles.

The VLS runs forward in time in conjunction with the filter producing smoothed estimates at historical epochs. Observations in the present are mapped back to a set of selected historical epochs sequentially until the estimates at those historical epochs are deemed to be “converged”. The relationship between filter and a single VLS epoch is illustrated in Figure 2. The set of historical epochs can be selected at any granularity based on a goal of being able to accurately interpolate the results. Convergence can be defined in many ways, but an intuitive method is to identify when the covariance on the smoothed estimate is no longer reduced significantly by the processing of new measurements. This study opts to identify a time lag which satisfies this criterion based on trial runs. The use of a static time lag, though potentially not optimal, is simpler to implement in an operational framework.

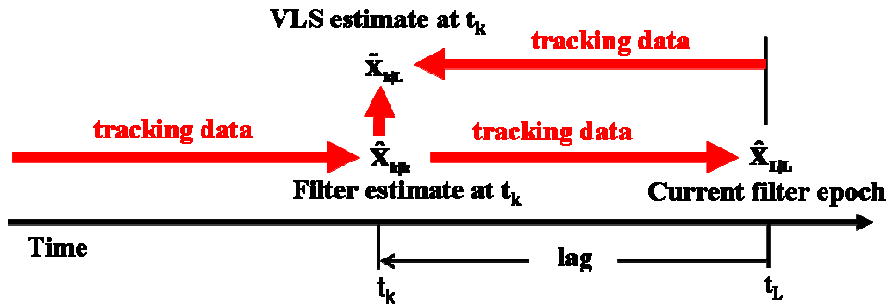


Figure 2. VLS incorporates current time observations into historical estimates.

Estimate Combination

The sequential filter and VLS both perform a large number of matrix operations. The computational expense of these operations increases significantly with increasing size of the state estimate. To partially offset the computational expense related to the large state size of a full simultaneous solution, this study experimentally separated a population of 75 calibration satellites into

three subsets of 25 satellites. The separation was performed roughly in terms of the satellite altitudes, resulting in high, medium and low altitude subsets. A final smoothed estimate of the global atmospheric density model correction states is constructed by combining the variable lag smoother estimates from the sub-set solutions.¹³ Common state and state-error covariance information from each sub-group solution is combined at each variable lag smoother epoch. The state estimate for the i^{th} filter has the structure

$$\hat{X}^i = \begin{bmatrix} \hat{x}^i \\ \hat{c}^i \end{bmatrix}, \quad (6)$$

where x^i are the states unique to the satellite orbits estimated in the i^{th} filter and c is a vector of parameters common to all satellites in all filters which includes the atmospheric density model correction states. The covariance of X^i is then partitioned as

$$P_X^i = \begin{bmatrix} P_{xx}^i & P_{xc}^i \\ P_{cx}^i & P_{cc}^i \end{bmatrix}. \quad (7)$$

We assume that all filters start with the same *a priori* information for the common states, which we designate as a mean estimate c_0 with covariance P_{cc}^0 . Common parameter estimates from individual estimation runs are combined by first computing the information matrix (the inverse of the covariance) and information vector as

$$\Lambda_{cc}^i \equiv [P_{cc}^i]^{-1}, \quad (8)$$

$$d_c^i \equiv \Lambda_{cc}^i \hat{c}^i. \quad (9)$$

Independent information is combined in information form through simple addition to produce the combined estimate and covariance. We note, however, that the solutions for the independent satellites are correlated through the use of common *a priori* information. The *a priori* information is therefore subtracted from each individual estimate and added back in once to remove this correlation:

$$\Lambda_{cc} = \Lambda_{cc}^0 + \sum_i [\Lambda_{cc}^i - \Lambda_{cc}^0], \quad (10)$$

$$d_c = d_c^0 + \sum_i [d_c^i - d_c^0], \quad (11)$$

where d_c^0 and Λ_{cc}^0 are the information vector and information matrix capturing the *a priori* information.* Finally, the combined estimate and covariance are computed as:

$$P_{cc} = [\Lambda_{cc}]^{-1}, \quad (12)$$

* One could alternatively not subtract the *a priori* information from one of the individual solutions.

$$\hat{c} = [P_{cc}]^{-1} d_c . \quad (13)$$

The described method for combining estimates can be applied to either filtered or smoothed estimates. For this study, smoothed solutions are combined for reasons provided above. It is important to note that this method of combining solutions is only strictly valid for cases where the common parameters are time constants. If the common parameters are time varying, as they are presumed to be for this application, the individual filter and smoother estimates will be correlated through common process model errors. This topic will be revisited in the sequel.

ANALYSIS

To explore the observability of the two temperature parameters currently estimated in the HASDM process, this analysis first examines the case where each temperature parameter correction is represented as a scalar, and then the analysis is extended to cases where low degree and order spherical harmonic expansions represent the temperature corrections. All simulation test cases are performed with a simulated set of 75 satellites tracked by SSN sensors, with the orbital distribution of the satellites in the simulation test set given in Table 1 in a manner consistent with published HASDM information.²

Table 1. Satellite orbit distribution.

Altitude Range (km)	<i>190-250</i>	<i>250-300</i>	<i>300-400</i>	<i>400-500</i>	<i>500-600</i>	<i>600-700</i>	<i>700-900</i>
Inclination (°)							
<i>20-30</i>	2	3	1				
<i>30-40</i>	5			1		1	
<i>40-50</i>	1		3	1	2	1	
<i>50-60</i>	1	1	1		1		
<i>60-70</i>			2	2			2
<i>70-80</i>		1	4				1
<i>80-100</i>		2	10	6	12	4	4
Total	9	7	21	10	15	6	7

T_x Scalar, T_c Scalar

Scalar representations of the nighttime minimum exospheric temperature, T_c , and the inflection point temperature at 125 km, T_x , were used in the generation of simulated time histories of the temperature parameters, shown in Figure 3. Use of a scalar representation is equivalent to the 0×0 spherical harmonic expansion where only its $C_{0,0}$ coefficient is estimated. Simulated tracking data were produced for all 75 satellites whose trajectories were computed using the deviated temperature profiles in the Jacchia 1970 atmospheric density model. The deviated temperature profiles are generated based on initial Gaussian random draws for each temperature correction coefficient which are transitioned through time using stochastic sequence defined by Equation 2. The resulting deviated temperature history generates perturbed densities when processed through the Jacchia 1970 atmospheric density model during orbit propagation. The resulting orbit trajectories

are then used in the generation of simulated tracking data. The initial simulation was run using a half-life of 3 hours, based on the frequency of reported geo-magnetic data and the current 3-hour segmented time constants in HASDM, for both temperature parameters. Based on published time histories of estimated temperature corrections, the one-sigma uncertainties on the T_c and T_x corrections are set to 50 K and 15 K respectively.³ Ballistic coefficient uncertainty was set to 3% for all satellites with a correlation half-life of 1×10^{10} minutes. Estimation was performed with the simulated tracking data using the sequential filter and the VLS with a maximum lag of 12 hours. Estimates of temperature correction from the VLS were generated on a 15-minute time grid.

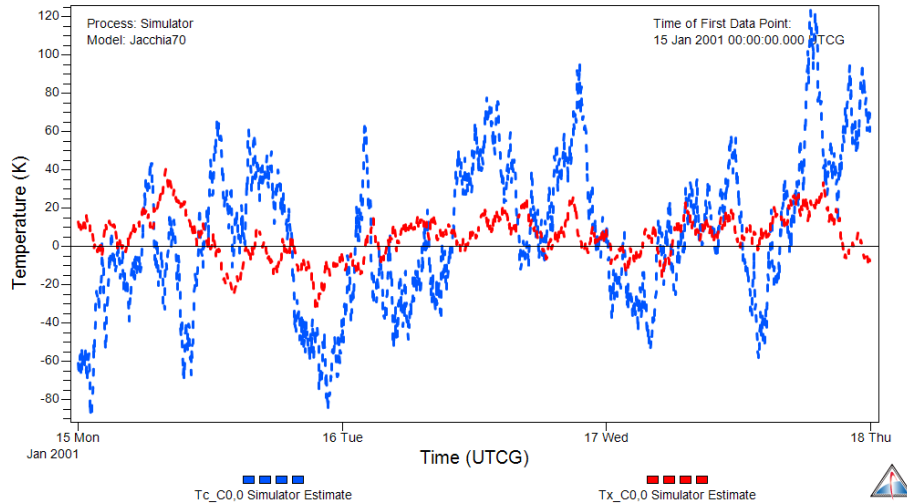


Figure 3. Simulated temperature correction profiles with 3-hour half-life.

The estimated temperature corrections from the VLS are illustrated with simulated time histories in Figure 4. The smoothed solution is in phase with the simulation, indicating that lag in the filter estimates have been sufficiently removed. Errors in the smoothed solution are displayed in Figure 5 along with associated 95% (2-sigma) probability bounds. The smoothed solutions for both temperature parameters are seen to be consistent with their formal uncertainties. This is an indication that the process of combining estimates is not adversely affecting the final solution. The degree to which the 2-sigma bounds are reduced from their *a priori* values (100 K for T_c , 30 K for T_x) is an indication of the observability of the parameter.

The uncertainty bounds on the temperature coefficients drop initially, remain at a fairly steady level for the majority of the run, and rise again at the end. This behavior may be best explained in reverse time order. Starting at the end of the estimation interval, the smoothed solution contains the same information as the filter solution. The uncertainty at the end time of the estimation interval therefore represents the steady state filter uncertainty. Estimates at earlier epochs in the smoother solution contain information from all historical measurements and from all future measurements that reside within the maximum lag of the VLS. The use of information from both sides of the smoothed solution point generates an improved solution relative to the filter solution.

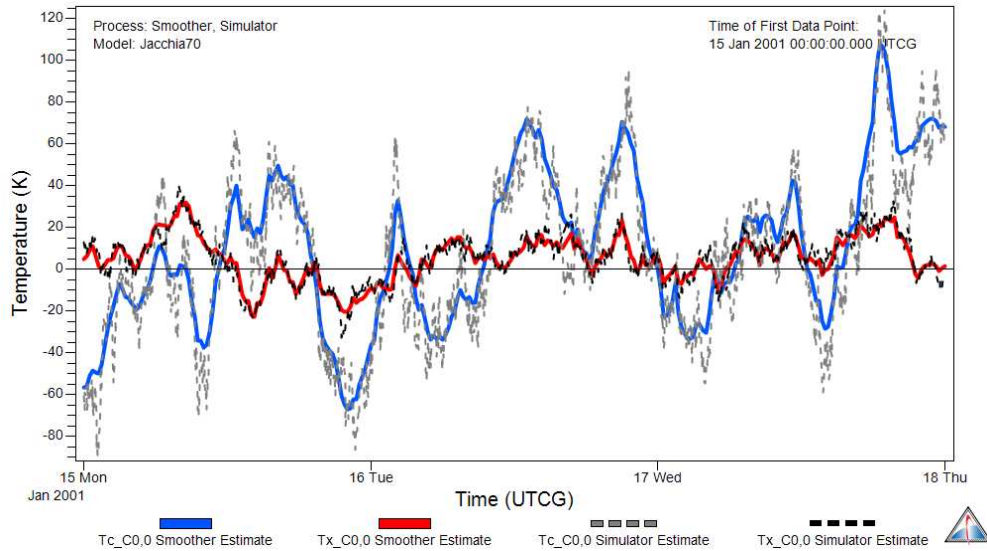


Figure 4. Estimated and simulated T_c and T_x correction profiles.

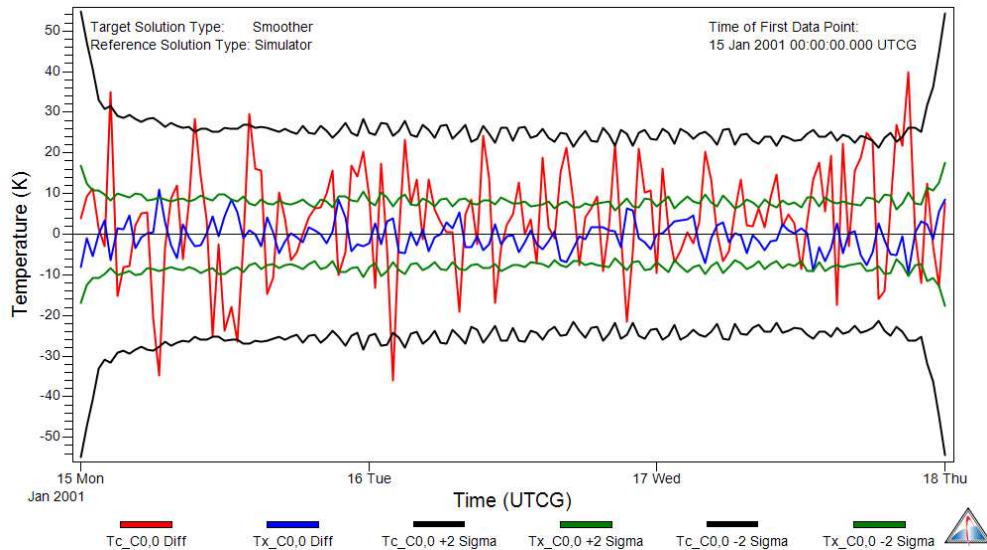


Figure 5. Errors in smoothed T_c and T_x correction estimates.

The higher uncertainty at the beginning of the run is an artifact of filter initialization (prior to the filter reaching steady-state performance) and will not be present operationally when filter runs are started using the full state and state error covariance from the end of the prior filter run. The time interval required for the smoother solution to reach a steady-state level moving backwards represents the latency of the smoothed solution: the lag relative to real time with which a *converged* smoothed solution is available. The VLS maximum lag was set to 12 hours. This is much longer than the time required to reach the smoother steady state uncertainty; thus the VLS maxi-

mum lag is not the driving the smoother uncertainty profile. In practice, the maximum VLS lag might be shortened to be slightly longer than latency period. As shown in Figure 6, a VLS lag of 2 hours appears adequate for this parameterization. To determine the effect of the chosen temperature correction half-life values on the required VLS lag, additional simulations were run with half-lives of 6 hours and 12 hours, with both resulting in the same VLS lag of 2 hours.

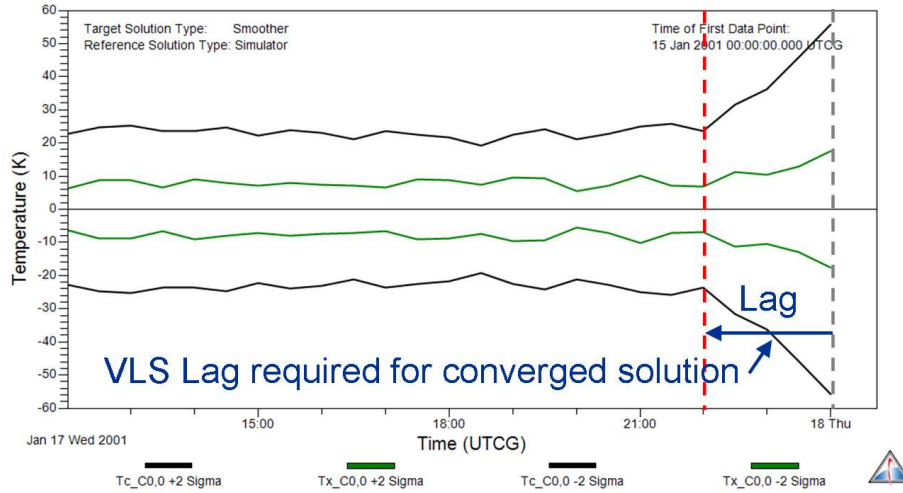


Figure 6. Selection of the maximum lag for the VLS.

The correlation of the T_c and T_x corrections from the smoother solution is shown in Figure 7. The strong negative correlation will be revisited as higher degree and order representations of the temperature corrections are analyzed. The correlations were examined for additional simulations using temperature correction half-lives of 6 and 12 hours. Comparing the results of the 3 runs, the correlation is noted to become slightly stronger as the half-life of the temperature estimates is lengthened.

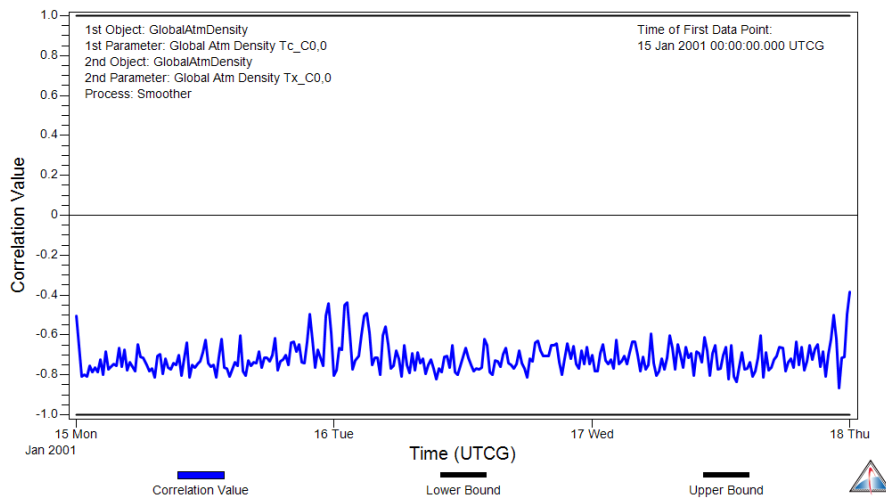


Figure 7. T_c - T_x cross-correlation

Part of the rationale for estimating corrections to two temperature parameters in HASDM is that T_c more strongly influences density at higher altitudes while T_x provides stronger influence at low altitudes.⁵ The relative observability of both T_c and T_x can be examined by plotting their respective formal uncertainties using the subsets of the 25 highest altitude satellites and the 25 lowest altitude satellites. These results are shown in Figure 8 and Figure 9, which display one-sigma uncertainties instead of two-sigma uncertainty bounds as shown in Figure 5. The reduction in uncertainty of T_c corrections is reduced by approximately 50% and 75% via estimation of the highest and lowest altitude satellite subsets respectively while analogous reduction in uncertainty of T_x corrections was approximately 14% and 75%. While both temperature parameters are highly observable based on the processing of low altitude satellites, T_x appears only marginally observable from higher altitude satellites.

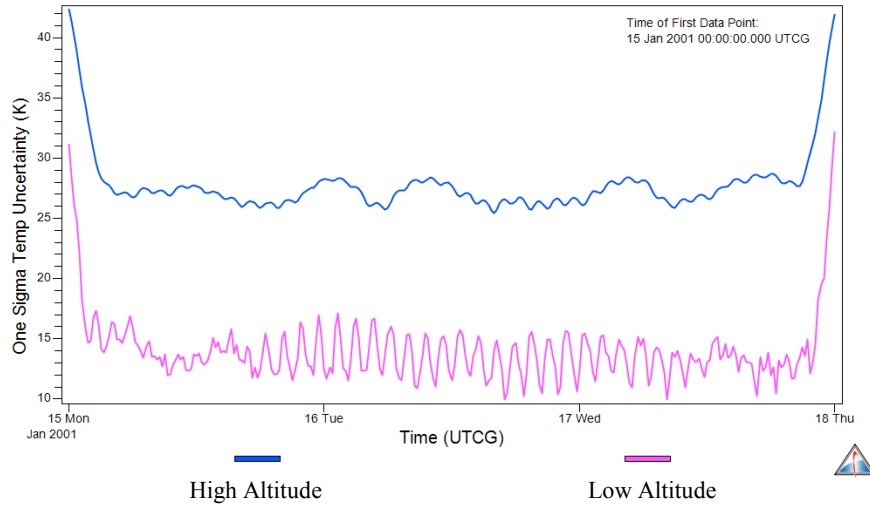


Figure 8. T_c uncertainty using subsets of high and low altitude satellites.

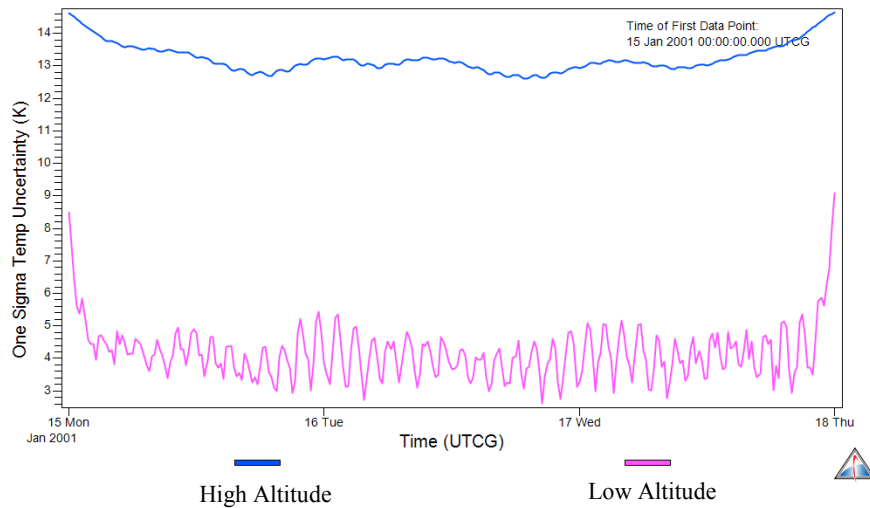


Figure 9. T_x uncertainty using subsets of high and low altitude satellites.

T_x Scalar, T_c 1×1

Changing the parameterization of corrections to T_c to be a 1×1 spherical harmonic expansion, the total number of estimated temperature correction coefficients becomes five: four for T_c , and one for T_x . Storz *et al.* indicate that the original segmentation of the temperature coefficients in HASDM was constructed to solve for updates to the $C_{0,0}$ terms every three hours while all other coefficients were updated every 12 hours.⁵ A more recent 2003 HASDM description states that all coefficients are updated every 3 hours, but autocorrelation constraints are placed on all coefficients using a 3 hour half-life for $C_{0,0}$ terms and an 18 hour half-life for all higher degree and order terms.²

For this study, $C_{0,0}$ terms are constrained using a 3-hour half-life while an 18-hour half-life is used for all other terms, out of consideration of the 2003 HASDM description. Lacking HASDM time histories for the additional T_c correction coefficients, one sigma uncertainties of 20 K are arbitrarily selected. Errors and error ratios for the smoothed estimates are shown in Figure 10 and Figure 11 respectively. *Error ratios* are defined as the error in the estimated parameter divided by its root variance. The horizontal lines at ± 3 in the error-ratio plot represent the 99% confidence interval. Once again the errors are mainly consistent with their formal uncertainties, although the estimate combination process causes a few significant excursions. The apparent lag of the converged smoothed solution from real time has not changed significantly from the scalar case. Correlations between the estimated coefficients were examined and one significant correlation, T_c $C_{0,0} - T_x$, was identified (Figure 12). This finding is also consistent with the correlation identified in the scalar case above.

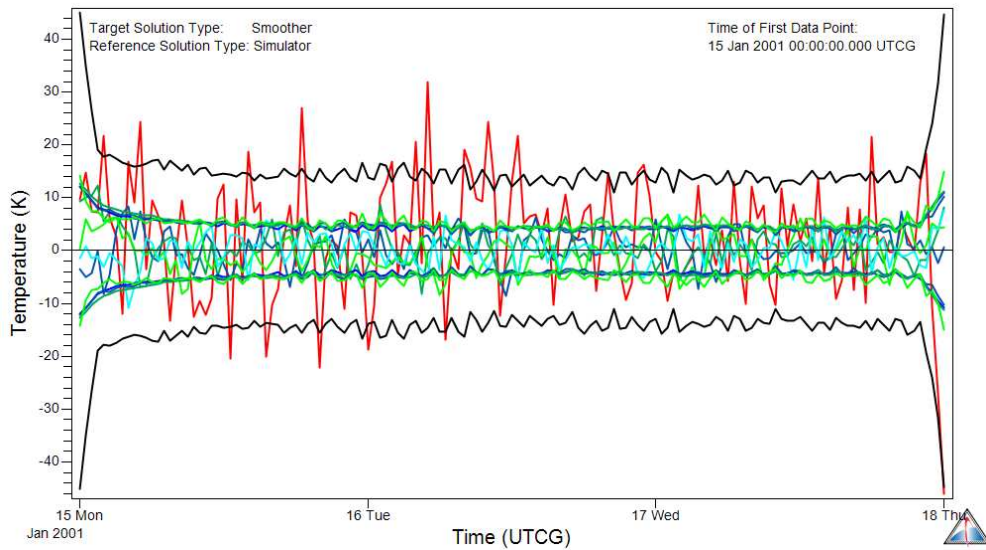


Figure 10. Errors in smoothed T_c 1×1 and T_x coefficient correction estimates.

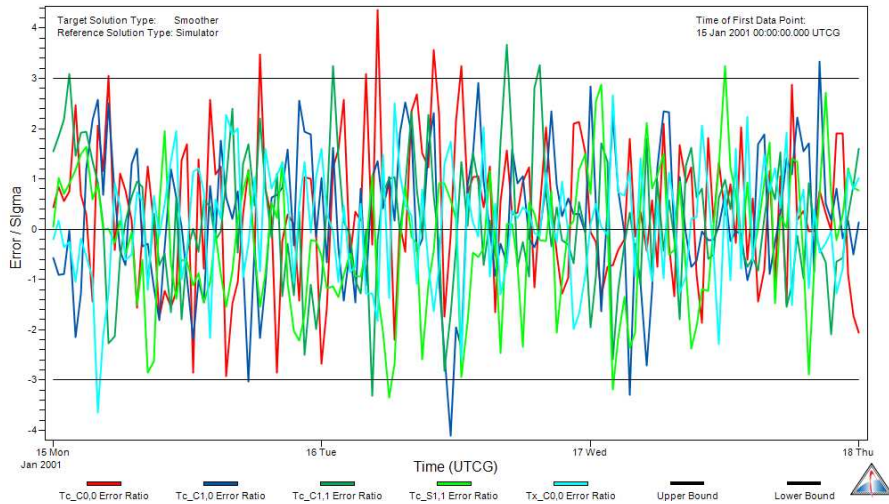


Figure 11. Error ratios for smoothed T_c 1×1 and T_x coefficient correction estimates.

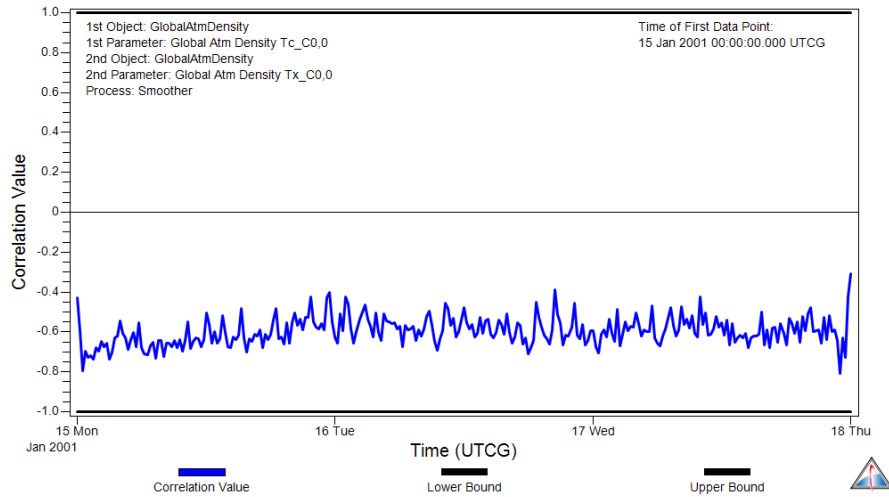


Figure 12. $T_c C_{0,0} - T_x$ cross correlation.

T_x 1×1 , T_c 2×2

The parameterization used operationally in HASDM is examined, modeled as a 2×2 spherical harmonic representation of corrections to T_c and a 1×1 spherical harmonic representation of corrections to T_x . The total number of estimated temperature correction coefficients is now thirteen: nine for T_c , and four for T_x . Excepting the $C_{0,0}$ coefficient, the *a priori* one-sigma uncertainty of 20 K for T_c coefficients is maintained. An *a priori* one sigma uncertainty value of 10 K is used for the T_x coefficients other than the $C_{0,0}$. Errors and error ratios for the smoothed temperature correction estimates are shown in Figure 13 and Figure 14 respectively. Again there are a few excursions where the errors are not consistent with the covariance, which is an artifact of the es-

time combination process. While undesirable, these excursions are not expected to result in a significant degradation in the overall accuracy of the solution. An examination of the smoother convergence reveals that while the solution is mostly converged at the 2-hour lag, some of the temperature corrections continue to reduce in uncertainty until the lag reaches approximately 6 hours. Further analysis is required to determine if there is a significant difference in orbit accuracy between the 2 and 6 hour lag solutions. Correlations between the estimated coefficients were examined and significant correlations were identified between all coefficients of like degree and order (Figure 16 through Figure 19). This result is consistent with the findings from the lower degree and order expansions analyzed above and results reported by Casali *et al.*³

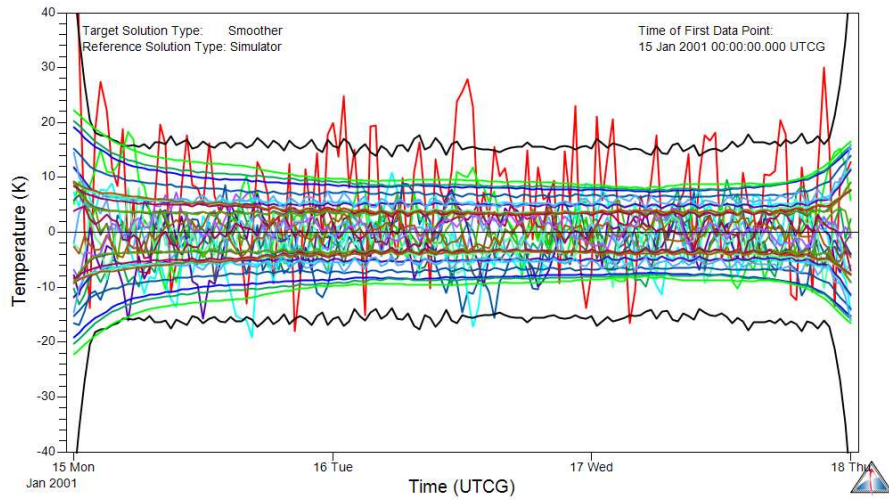


Figure 13. Errors in smoothed T_c 1×1 and T_x 2×2 coefficient correction estimates.

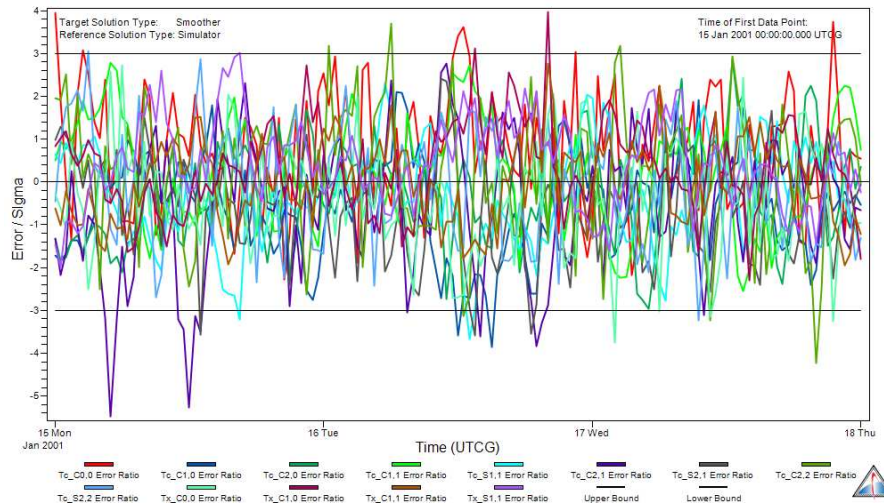


Figure 14. Error ratios for smoothed T_c 1×1 and T_x 2×2 coefficient correction estimates.

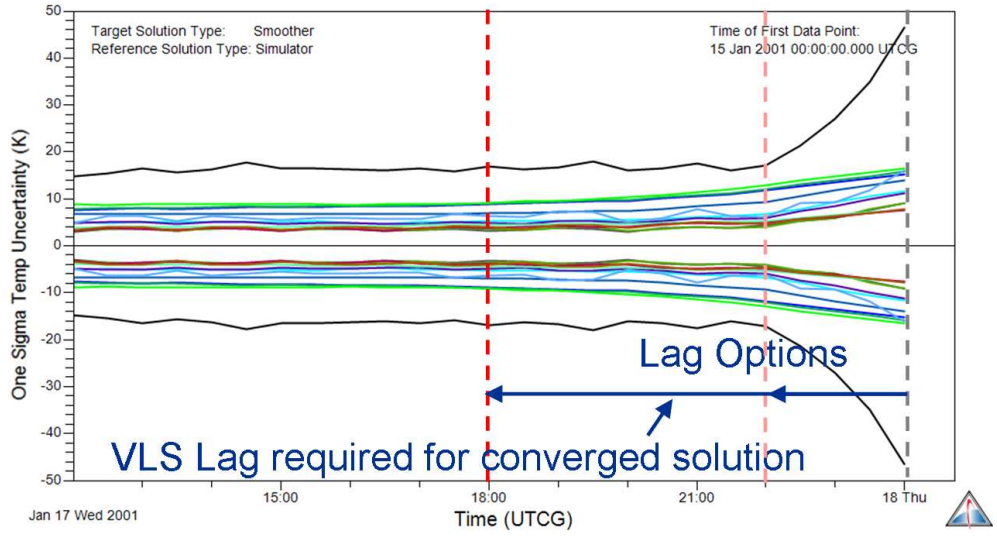


Figure 15. Selection of the maximum lag for the VLS (T_c 1x1, T_x 2x2)

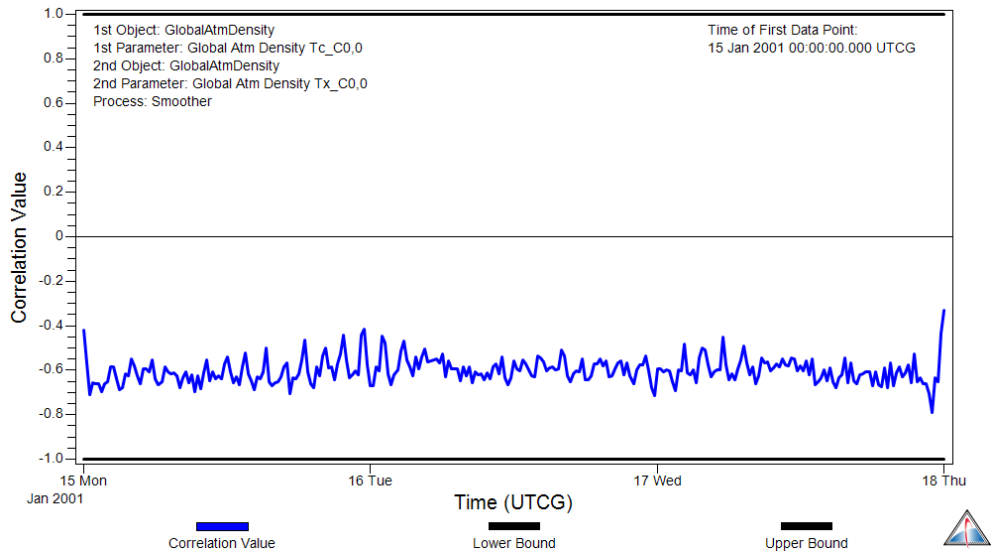


Figure 16. $T_c C_{0,0} - T_x C_{0,0}$ cross correlation.

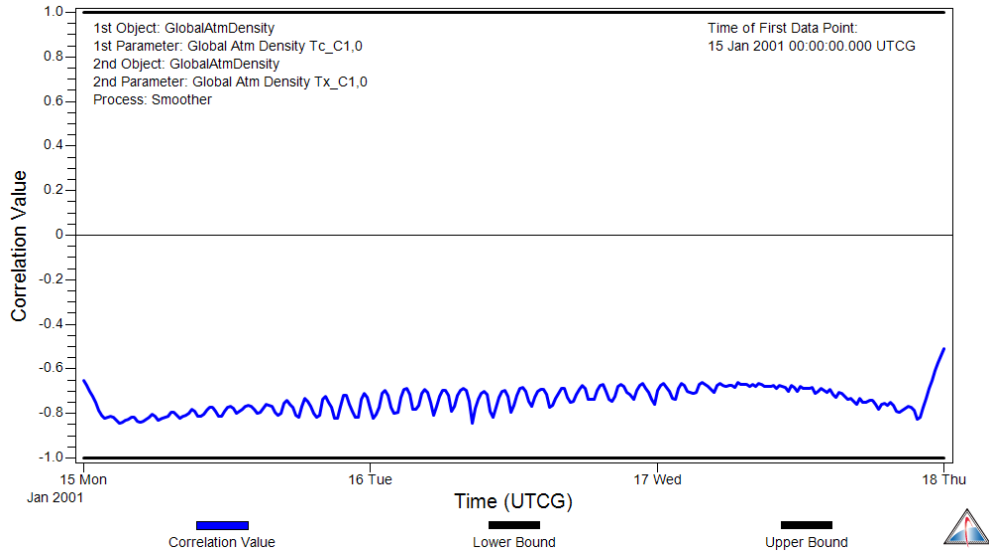


Figure 17. $T_c C_{1,0} - T_x C_{1,0}$ cross correlation.

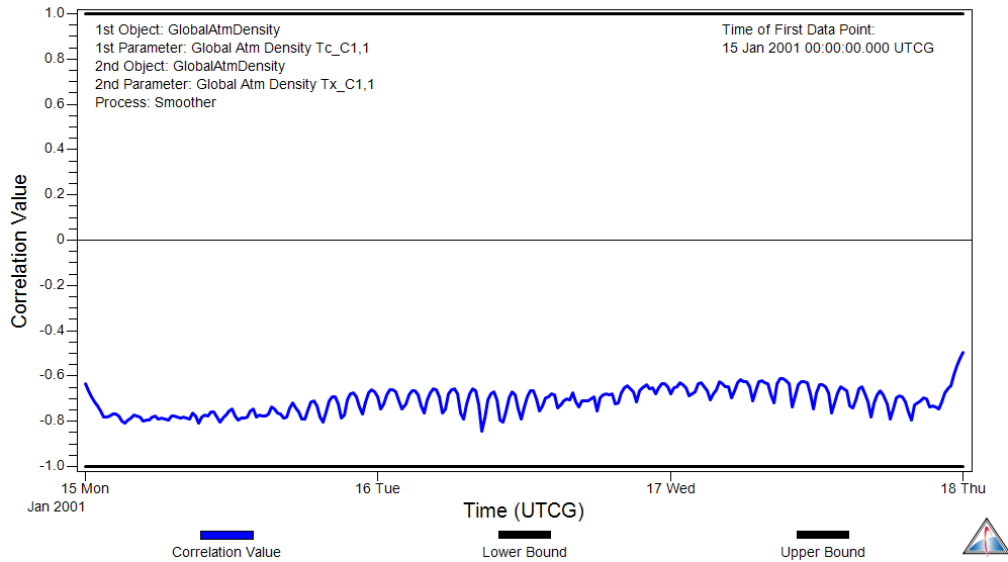


Figure 18. $T_c C_{1,1} - T_x C_{1,1}$ cross correlation.

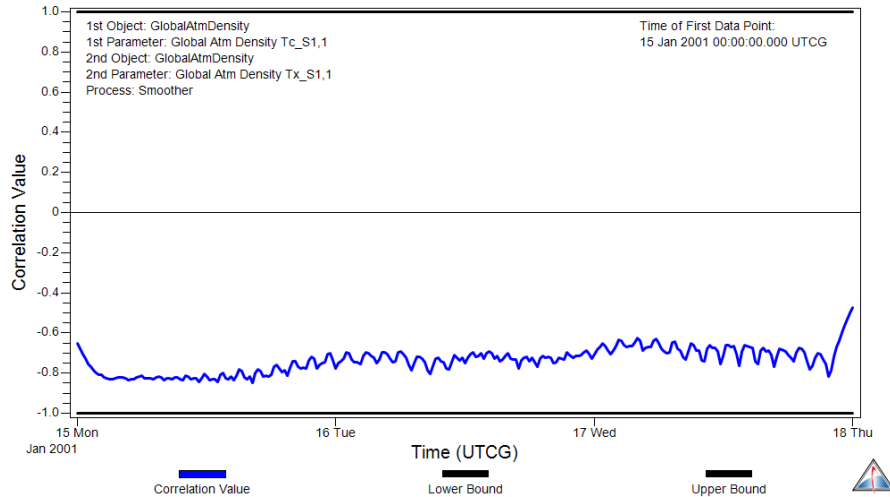


Figure 19. $T_c S_{1,1} - T_x S_{1,1}$ cross correlation.

CONCLUSION

Sequential estimation has been shown to be viable for the estimation of corrections to a global atmospheric density model. Performance of the estimation algorithms with simulated data is as expected and appears to track temperature variations over short time periods. The process of combining estimates from three (3) smoothed solutions is seen to produce a small number of artifacts where solution errors are inconsistent with the covariance function, but in the opinion of the authors their magnitude is not enough to be of significant concern. The specific parameterizations of the correction model were chosen to be consistent with the operational capability of AFSPC because published results were available and this could facilitate future comparisons. However, the estimation architecture in ODTK is general in nature, supporting alternative parameterizations.

The application of sequential estimation technology to the estimation of corrections to a global atmospheric density model has the desirable characteristics of:

- producing a continuous time history of corrections without the need for solution segmentation,
- eliminating fit-span considerations, as estimation always starts with the final state and state error covariance from the prior run and processes only new observations, and
- identifying the latency with which converged solutions are available for space-object catalog orbit determination.

The logical next steps in evaluating the application of sequential estimators to correct global-density models are to evaluate orbit accuracy improvement for resident space objects outside of the calibration set, evaluate the effect of additional satellites on solution latency and observability, and test the capability using real data.

REFERENCES

- ¹ Casali, S.J., Barker, W.N., “Dynamic Calibration Atmosphere (DCA) for the High Accuracy Satellite Drag Model (HASDM),” Paper AIAA-2002-4388, AIAA/AAS Astrodynamics Specialist Conference, Monterey, CA, August 2002.
- ² Bowman, B. R., and Storz, M.F., “High Accuracy Satellite Drag Model (HASDM) Review”, Paper AAS 03-625, from de Lafontaine, J., et al. (eds.), *Astrodynamics 2003 - Advances in the Astronautical Sciences*, Vol. 116, Part III. Proceedings of the AAS/AIAA Astrodynamics Specialist Conference, Big Sky, Montana, August 2003. pp. 1943-52.
- ³ Casali, S.J., Barker, W.N., Bowman, B. R., “Improvements in Density Modeling Using the Air Force Dynamic Calibration Atmosphere Model,” Paper AIAA-2006-6168, AIAA/AAS Astrodynamics Specialist Conference, Keystone, CO, August 2006.
- ⁴ Gabor, M.J., “An Independent Technical Review Process for Government Developed Models: HASDM as a Case Study,” AAS 05-200, AAS/AIAA Space Flight Mechanics Meeting, Copper Mountain, Colorado, January 2005.
- ⁵ Storz, M.F., Bowman, B.R., Branson, J.I., “High Accuracy Satellite Drag Model (HASDM),” AIAA 2002-4886, AIAA/AAS Astrodynamics Specialist Conference, Monterey, California, August 2002.
- ⁶ Wright, J.R., “Real-Time Estimation of Local Atmospheric Density.” Paper AAS 03-164, from Scheeres, D.J. *et al.* (eds.), *Spaceflight Mechanics 2003-Advances in the Astronautical Sciences*, Vol. 114, Part II, Proceedings of the 13th AAS/AIAA Space Flight Mechanics Meeting, Ponce, Puerto Rico February 9-13, 2003, pp. 927-50.
- ⁷ Wright, J.R., Woodburn J.W., “Simultaneous Real-Time Estimation of Atmospheric Density and Ballistic Coefficient.” Paper AAS 04-175, from Coffey, S.L., *et al.* (eds.), *Spaceflight Mechanics 2005 – Advances in the Astronautical Sciences*, Vol. 119, Part II, Proceedings of the 14th AAS/AIAA Space Flight Mechanics Conference, Maui, Hawaii, February 8-12, 2004, pp. 1155-84.
- ⁸ Wright, J.R. (2002), “Optimal Orbit Determination.” Paper AAS 02-192, from Alfriend, K.T., *et al.* (eds.), *Spaceflight Mechanics 2002 - Advances in the Astronautical Sciences, Vol. 112, Part II*, Proceedings of the AAS/AIAA Space Flight Mechanics Meeting, San Antonio, Texas, January 27-30, 2002, pp. 1123-34.
- ⁹ Wright, J.R., Woodburn, J., “Nonlinear Variable Lag Smoother,” AAS 08-303, AAS/AIAA Space Flight Mechanics Meeting, Galveston, Texas, February 2008.
- ¹⁰ Vallado, D., Hujak, R., Johnson, T., Seago, J. and Woodburn, J., “Orbit Determination Using ODTK Version 6,” 4th International Conference on Astrodynamics Tools and Techniques, European Space Astronomy Centre, Madrid 2010.
- ¹¹ Jacchia, L.G., “New Static Models of the Thermosphere and Exosphere with Empirical Temperature Profiles,” SAO Special Report No. 313, Smithsonian Institution Astrophysical Observatory, May 1970.
- ¹² Tanygin, S., Wright J.R. ,“Removal of Arbitrary Discontinuities in Atmospheric Density Modeling.” Paper AAS 04-176, from Coffey *et al.* (2004), *Spaceflight Mechanics 2004 - Advances in the Astronautical Sciences*. Vol. 119, Part II, Proceedings of the 14th AAS/AIAA Space Flight Mechanics Meeting, Maui, Hawaii, February 8-12, 2004, p. 1186?.
- ¹³ McReynolds, S., “Combining Estimates of Common Parameters from Many Kalman Filters”, AGI Internal Memo.